WILEY JCN

RESEARCH ARTICLE

Quantifying the relationship between optical anatomy and retinal physiological sensitivity: A comparative approach

Robert F. Rosencrans[1] | Caitlin E. Leslie[2] | Keith A. Perkins[1] | Whitney Walkowski[1] |
William C. Gordon[1,3] | Corinne L. Richards-Zawacki[4] | Nicolas G. Bazan[1,3] |
Hamilton E. Farris[1,5,6]

[1]Neuroscience Center, Louisiana State University School of Medicine, New Orleans, Louisiana

[2]Department of Integrative Biology, University of Texas, Austin, Texas

[3]Department of Ophthalmology, Louisiana State University School of Medicine, New Orleans, Louisiana

[4]Department of Biological Sciences, University of Pittsburgh, Pittsburgh, Pennsylvania

[5]Department of Otorhinolaryngology, Louisiana State University School of Medicine, New Orleans, Louisiana

[6]Department of Cell Biology and Anatomy, Louisiana State University School of Medicine, New Orleans, Louisiana

Correspondence
Hamilton E. Farris, Neuroscience Center, Louisiana State University School of Medicine, 2020 Gravier Street, New Orleans, LA 70112, USA.
Email: hfarri@lsuhsc.edu

Abstract

Light intensity varies 1 million-fold between night and day, driving the evolution of eye morphology and retinal physiology. Despite extensive research across taxa showing anatomical adaptations to light niches, surprisingly few empirical studies have quantified the relationship between such traits and the physiological sensitivity to light. In this study, we employ a comparative approach in frogs to determine the physiological sensitivity of eyes in two nocturnal (*Rana pipiens*, *Hyla cinerea*) and two diurnal species (*Oophaga pumilio*, *Mantella viridis*), examining whether differences in retinal thresholds can be explained by ocular and cellular anatomy. Scotopic electroretinogram (ERG) analysis of relative b-wave amplitude reveals 10- to 100-fold greater light sensitivity in nocturnal compared to diurnal frogs. Ocular and cellular optics (aperture, focal length, and rod outer segment dimensions) were assessed via the Land equation to quantify differences in optical sensitivity. Variance in retinal thresholds was overwhelmingly explained by Land equation solutions, which describe the optical sensitivity of single rods. Thus, at the b-wave, stimulus-response thresholds may be unaffected by photoreceptor convergence (which create larger, combined collecting areas). Follow-up experiments were conducted using photopic ERGs, which reflect cone vision. Under these conditions, the relative difference in thresholds was reversed, such that diurnal species were more sensitive than nocturnal species. Thus, photopic data suggest that rod-specific adaptations, not ocular anatomy (e.g., aperture and focal distance), drive scotopic thresholds differences. To the best of our knowledge, these data provide the first quantified relationship between optical and physiological sensitivity in vertebrates active in different light regimes.

KEYWORDS

bipolar cells, dendrobatidae, diel, diurnal, electroretinogram, frog, nocturnal, photoreceptors, retina, sensitivity, sensory ecology

1 | INTRODUCTION

Anurans diverged from urodeles and caecilians approximately 265 million years ago, diversifying into a variety of habitats (Zhang et al., 2005), including aquatic, desert, and forest floor and/or canopy environments (Duellman & Trueb, 1994; Wells, 2007). Although all of these environments vary in the intensity and spectral content of light (Nascimento, Amano, & Foster, 2016), the variance between habitats

is dwarfed by light differences created by the diel cycle, in which a million-fold difference in light intensity is observed between day and night (Land & Nilsson, 2002; Nascimento et al., 2016). How has this diversity in visual ecology affected the visual anatomy and physiology of species in these different light regimes? Sensory ecology (Dusenbery, 1992; Endler, 1992) predicts that dramatic variance in light environments should select for dramatic differences in the visual system (Warrant & Johnsen, 2013). In particular, low photon numbers

associated with nocturnal behavior may select for optical and physiological traits that increase sensitivity to dim light (e.g., larger rod outer segments; short focal length eyes, and large pupils). Alternatively, the bright light of diurnal ecology may relieve evolutionary pressure toward increased sensitivity, allowing eyes to evolve traits that enable higher spatial resolution driven by large focal length eyes with cone-dominated photoreceptor mosaics (Cronin, Johnsen, Marshall, & Warrant, 2014). The relationship between optical traits and sensitivity per receptor was formalized by Land (1981) in Equation (1), which calculates sensitivity (S) to white light as the ratio of photons absorbed by a photoreceptor to those emitted within a steradian (sr) of solid angle of an extended source (Warrant & Dacke, 2011),

$$S = \left(\frac{\pi}{4}\right)^2 (A)^2 \left(\frac{d}{f}\right)^2 \left(\frac{kl}{2.3+kl}\right) \qquad (1)$$

where A is the aperture, f is the focal length, and d and l are the diameter and length of a rod outer segment, respectively (Land, 1981; Land & Nilsson, 2002; Warrant & Nilsson, 1998). k represents the absorption coefficient or the proportion of photons absorbed per unit length of the photoreceptors. The units for S are μm^2 sr. The equation shows that as pupillary diameter increases, fewer incoming photons are reflected or absorbed by the pigmented iris. This effect increases sensitivity to dim light and forms the mechanism by which mydriasis enhances sensitivity. Photons which pass through the pupil are in turn focused by the lens onto a discrete number of photoreceptors. The focal length (f) determines the area of the retina over which the stimulus is distributed. This area is converted to a number of receptors when the focal length is considered together with receptor cell diameter to form the acceptance angle (d/f). Small acceptance angles spread the photons from a given part of the visual field over more photoreceptors, decreasing per receptor sensitivity while enhancing resolution. Conversely, large acceptance angles concentrate light from a given area on to fewer photoreceptors, enhancing sensitivity while decreasing resolution. Thus, focal length and pupillary diameter exponentially and equally affect sensitivity in opposite directions. Like outer segment diameters (d), increased photoreceptor length (l) also enhances sensitivity by increasing the probability of photon capture in individual rods. In the Land equation, the effect of photoreceptor length is scaled by the probability of photon absorption per unit length (k). Given that the Land equation describes the optical sensitivity of any eye of a given gross morphology (A, f) and a set of photoreceptor characteristics (d, l, k), numerous studies across disparate taxa have made morphological measurements in harvested tissue to calculate expected eye sensitivity (Land & Nilsson, 2002). However, to the best of our knowledge, the direct relationship between these optical traits and actual retinal physiological sensitivity has received surprisingly little attention across species with different morphologies, having been tested only in invertebrates (Frederiksen & Warrant, 2008). Thus, in the present study, we determined the relationship between optical anatomy and retinal physiological sensitivity to light in two nocturnal and two diurnal species of frogs: *Hyla cinerea* (nocturnal), *Rana pipiens* (nocturnal), *Oophaga pumilio* (diurnal), and *Mantella viridis* (diurnal). Using histological techniques in conjunction with in vivo electroretinograms (ERGs) and infrared photography, the experiments presented here test the extent to which optical and cellular

parameters explain electrophysiological sensitivity under scotopic and photopic conditions. Furthermore, by quantifying the relationship between optical and physiological sensitivity, our data are predictive of luminance thresholds for eyes of any anatomy.

2 | MATERIALS AND METHODS

2.1 | Animals

All experiments were approved by the Institutional Animal Care and Use Committee of Louisiana State University Health Sciences Center, New Orleans. *Hyla cinerea* was wild caught by the authors (permitted by Louisiana DWF) or a vendor (Snakes at Sunset; Miami, FL). *Rana pipiens* were purchased from vendors (Sullivan Co., Nashville, TN; Carolina Biological Supply Company; Burlington, NC). *Oophaga pumilio* were captive-bred (Richards-Zawacki Laboratory, Pittsburgh, PA). Captive-bred *Mantella viridis* were purchased from a vendor (Josh's Frogs LLC, Owosso, MI). Although species may exhibit continuous changes in activity across different points in the diel cycle, the subject species were classified as either nocturnal or diurnal based on mating behavior (e.g., calling and phonotaxis). Whereas *H. cinerea* and *R. pipiens* are nocturnal (Garton & Grandon, 1975; Larson, 2004), *O. pumilio* and *M. viridis* are diurnal (Prohl & Hodl, 1999; Schaefer, Vences, & Veith, 2002; Summers, Symula, Clough, & Cronin, 1999). All animals were housed individually, fed ad libitum and kept on a 12:12 light/dark cycle (300 cd/m^2). No gravid females were tested. For histological assays, tissue was harvested from animals that were euthanized using 150 mg/kg intramuscular ethyl 3-aminobenzoate (Tricaine methanesulfonate; MS-222; Sigma Aldrich) followed by decapitation. If necessary, animals were sexed postmortem.

2.2 | ERG recordings

After 12–14 hr dark adaptation in a light-tight box, frogs were immobilized under dim red light (650 nm) using intramuscular succinylcholine chloride (150 mg/kg; Sigma Aldrich; St. Louis, MO) and placed dorsal side up in an Espion Ganzfeld Dome (Diagnosys LLC; Lowell, MA). The dome and recording apparatus were contained within a light-tight Faraday cage kept at 22.6 °C. Cutaneous respiration was maintained using a damp towel. Atropine sulfate (1%) was applied to both eyes for pupil dilation. Subdermal needle electrodes (GRASS Technologies, West Warwick, RI or Chalgren Enterprises, Gilroy, CA), inserted over the skull vertex and in the hind leg (e.g., toe pad), recorded the indifferent and ground signals, respectively. ERGs were recorded using silver silver-chloride electrodes (0.008 in. o.d.) placed on the cornea of both eyes for separate two-channel recordings. The scotopic ERG procedure began after an additional 6 min of dark adaptation in the dome. Subsequently, ERG responses to 1 ms flashes were measured at 21 different light intensities (0–2,000 cd s/m^2) in increasing quasi-logarithmic steps, with four flashes at each intensity. There was no background illumination in scotopic tests. For photopic ERGs, a constant background light (1.45 log cd/m^2) illuminated the dome throughout the procedure including the initial 6 min of adaptation time. The background light intensity was chosen to be within the

range of diurnal light intensities in the tropical forest floor habitat of diurnal frogs (Jaeger & Hailman, 1981). The intensity of photopic flashes ranged over 16 steps (0–3,000 cd s/m^2). To prevent adaptation during all ERGs, inter-flash intervals (5–120 s) as well as the interval between intensity steps (30–120 s) increased with light intensity. Subjects were monitored at all times in the dome using an infrared closed-circuit camera to make sure no movement altered electrode position. Light stimuli were produced by an LED or Xenon strobe source. ERG responses were filtered (high-pass 0.15 Hz; low-pass 100 Hz) and digitized for later analysis.

2.3 | ERG analysis

Using the recording from the eye with the highest signal-to-noise ratio throughout the procedure, b-wave amplitude was defined as the maximum voltage (measured from 0 V) between 50 and 400 ms following the flash. This large range was based on preliminary data to avoid peak discrimination at oscillatory potentials and parts of the c-wave. Because amplitude was measured from 0 V, responses to no light were used to correct for any drift that may have occurred in individual recordings. The no light recordings also enabled calculation of baseline noise (rms amplitude) used in b-wave peak discrimination. The response at each light intensity was the average b-wave amplitude to four flashes. Note, however, that in a small number of cases the average response was based on fewer flashes because a response to a flash was rejected due to one of the following criteria: (a) electrode became uncoupled to the cornea; (b) the peak discrimination routine solved for a voltage that was less than two standard deviations of the mean electrical activity (voltage) recorded in absence of light (baseline noise); and (c) spurious noise prevented traces from exhibiting an a- and/or b-wave. Given that absolute b-wave amplitude varied between individuals (e.g., due to electrode resistance; resistance of the ocular media including the lens, vitreous, and epithelium) each individual's intensity response function, or V-Log(I) curve, was normalized to its maximum to generate a relative response bound by 0 and 1 (Miller & Dowling, 1970), which was analyzed using a least-squares fit of the standard Boltzmann function.

$$\text{Relative b-wave amplitude} = \frac{A_1 - A_2}{1 + e^{\frac{(flash - flash_0)}{\tau}}} + A_2$$

Here, A_1 and A_2 equal 0 and 1, respectively, or the amplitudes at the beginning and end of the function; $flash$ is the Log of the light intensity stimuli at each step; the unknown variables are $flash_0$, the light intensity eliciting a 50% response; and τ, the slope of the function. Using this function enabled comparisons of the response thresholds (i.e., flash intensity eliciting a 10% response) and slopes across species (Eguchi & Horikoshi, 1984). Analysis of a-wave amplitude is not included here because a-wave responses to low-intensity stimuli that clearly elicited a response in the b-wave were often statistically near the noise level of the recording system. This had the potential to incorrectly estimate thresholds (i.e., too high), which was a critical metric in this study, as thresholds are not only used to compare between species here but also in the discussion of data collected in behavioral tests and measured light levels in the field.

2.4 | Outer segment dimensions

Following minimum overnight fixation in Karnovsky's fixative (2% glutaraldehyde, 2% formaldehyde, 0.135 M sodium cacodylate buffer; Electron Microscopy Sciences; Hatfield, PA), sections of the retina were rinsed with buffer and postfixed in cacodylate buffered 1% osmium tetroxide (Electron Microscopy Sciences) for 1 hr. After dehydration (ethanol followed by acetone) retina were infiltrated with 1:1 acetone to epoxy (Embed-812/araldite mixture) resin overnight. After overnight polymerization in plastic blocks, they were sectioned (1 μm) and subsequently stained with 1% w/v aqueous toluidine blue and sodium borate for bright field imaging (100×). Although many outer segments could be measured in a single section, retinas used in this assay were taken from a minimum of three individuals for each species (n = 3 [H. cinerea], 3 [R. pipiens], 5 [O. pumilio], and 3 [M. viridis]). All measurements were taken in the central portions of the retina within 20° of the optic disk and likely limited to the so-called red rods (i.e., with an outer segment longer than the inner segment; Donner & Reuter, 1976; Walls, 1942). Because the use of 1 μm sections could miss the widest portion of the cell and incorrectly estimate cell dimensions, measurements were independently confirmed by preparing retinal slices from different individuals and viewed using differential interference contrast (DIC) imaging. For the DIC procedure, outer segment length and width were taken from eyes fixed in 4% paraformaldehyde in PBS, cryoprotected in an ascending sucrose gradient (10, 20, and 30% sucrose in PBS) and subsequently frozen in media (Scigen Tissue Plus Optimum Cutting Temperature; O.C.T). After drying, 20–60 μm thick sections were wet mounted with PBS. Photoreceptor dimensions were then determined using a 60× water immersion objective under differential interference contrast using an Olympus BX51 (Tokyo, Japan) microscope. Note that although DIC did allow for changing focal plane to observe the largest cellular cross-section, it also presented a problem in that accurate determination of the outer segment membrane location could be obscured by neighboring cell segments. Nevertheless, comparison of the two methodologies revealed no difference in the dimension measures (t test; outer segment diameter plastic n = 92 vs. frozen DIC n = 42, p = .185; outer segment length plastic n = 86 vs. frozen DIC n = 45, p = .223). Thus, for consistency and having two independent and consistent measures, outer segment dimensions presented in the results and used in calculations of sensitivity were analyzed from plastic embedded preparations.

2.5 | Focal length

One eye from each specimen was extracted and fresh-frozen in media (OCT compound) submerged in liquid nitrogen. The eyes were then sectioned (20–60 μm thick) at −20 °C (Shandon Cryotome; Thermo Scientific, Waltham, MA). After staining (toluidine blue; see above), focal lengths and lens widths were obtained from sections exhibiting the widest lens (i.e., the center of the structure). Measurements were made using a calibrated eyepiece reticule at 2× magnification. Focal length was measured as the distance from the center of the lens to the interface of photoreceptor outer segments and inner segments.

2.6 | Infrared photography of pupillary diameter

After a minimum of 2 hr dark adaptation (<0.1 lx; Extech HD450 photometer), cornea were treated with 1% atropine sulfate (Sigma Aldrich, St. Louis, MO). Dilated pupils were then imaged using the 2007 Heidelberg Spectralis infrared camera (Heidelberg Engineering, Carlsbad, CA) and scaled with a ruler in the same focal plane as the pupil. Images were later scored using software calipers (Heidelberg 6 software). To account for elliptical pupils, the pupillary diameter was calculated as the average of the major and minor periods. The pupillary diameter and focal length measurements were measured from the same eyes (i.e., pre- and post-mortem, respectively).

2.7 | Statistical analyses

Normalized ERG V-Log(I) curves were analyzed using a least squares fit of the Boltzmann function, which is appropriate for data that vary between 0 and 1. The fits explained a significant portion of each response's variance ($p < .00001$ for each individual) and enabled calculation of the light intensity eliciting responses with 10 and 90% of the maximum amplitude (i.e., the threshold and saturation points, respectively), as well as calculation of the function's slope and dynamic range. Statistical significance of differences in the means of V-Log(I) parameters, as well as the optical anatomy measures, were assessed using the general linear model (SAS) and Tukey post hoc test with correction for multiple comparisons (Zar, 1999). Each individual threshold is used in five different comparisons: between sexes within species (female to male; 1); between species (e.g., Hc to Rp, Hc to Op, Hc to Mv; 3), between light regimes (nocturnal to diurnal; 1).

3 | RESULTS

3.1 | Scotopic ERGs

ERGs in all species conformed to the typical waveform (Figure. 1a), exhibiting a- and b-waves resulting from the responses of photoreceptors and bipolar cells, respectively (Pugh, Falsini, & Lyubarsky, 1998; Robson & Frishman, 1998). When b-wave amplitude (V) is normalized to the maximum amplitude response for each individual, V-Log(I) curves exhibited sigmoidal change with increasing light intensity (I) (Figure 1b). Thus, least-squares Boltzmann fits of each individual curve enabled extrapolation of the mean b-wave threshold (light intensity eliciting 10% Boltzmann response) and slope (τ) for each species (Figure 2a). For scotopic conditions examining rod driven activity, mean thresholds in nocturnal frogs, *H. cinerea* and *R. pipiens*, were significantly lower (1.4 orders of magnitude) than those in diurnal species *O. pumilio* and *M. viridis* (Figure 3a; Tables 1 and 2). Comparisons of thresholds within light regimes showed that within nocturnal species scotopic thresholds did not differ. In contrast, for diurnal species, the *O. pumilio* threshold was 0.7 orders of magnitude less sensitive than that for *M. viridis* (Table 2). With regard to V-Log(I) slope, compared to diurnal species, the nocturnal species had a more gradual change in response (Figure 2a; Tables 1 and 2), which created a significantly greater dynamic range (Tables 1 and 2). The increased dynamic range can be attributed to the differing thresholds (Tables 1 and 2) and

comparable saturation points for nocturnal and diurnal species. The Boltzmann slope and the dynamic range necessarily have identical variance, resulting in matched statistical analyses. Nevertheless, in the tables, we report both metrics for clarity in evaluating the range of light sensitivity. There were no differences between males and females for scotopic ERG measures (Table 3).

3.2 | Photopic ERGs

To assess species differences in cone sensitivity, photopic ERGs were conducted under a constant background adapting light of 1.45 log cd/m^2. All thresholds shifted to similar higher light intensities, such that there was a smaller range of thresholds than those measured under scotopic thresholds (Table 2). In contrast to scotopic conditions, however, nocturnal species were less sensitive than diurnal frogs (Figures 2b and 3b, Table 1). Similar to the scotopic results, intra-diel comparisons indicate that thresholds in nocturnal species do not differ from one another. Furthermore, within the diurnal species, *M. viridis* again exhibited lower thresholds than *O. pumilio* (Figures 2b and 3b; Table 2). There were no differences between males and females for photopic ERG measures (Table 3).

3.3 | Calculating sensitivity from morphological parameters

To test the strength of the relationship between physiological sensitivity and optical sensitivity, each anatomical parameter of the Land sensitivity equation was measured. First, pupillary diameters (*A*: aperture) and focal lengths (*f*) were determined using infrared photography and flash-frozen ocular sections, respectively (Figure 4a,b). Nocturnal frogs have larger pupils and focal lengths than those in diurnal frogs (Figure 4c; Tables 1 and 2). Comparisons within nocturnal and diurnal species indicate that while the two diurnal species did not differ in either ocular variable, in the nocturnal group *R. pipiens* exhibited a larger pupil and focal length than *H. cinerea* (Figure 4c; Table 2). As pupil diameter increases, more light is admitted, and sensitivity is enhanced through more photon capture. However, if the focal length is proportionally increased, photons are spread across more photoreceptors, decreasing sensitivity in equal measure (Figure 4d). Thus, if the eyes from different species scale isometrically, no effect on sensitivity will be observed. For this reason, variance in these parameters as individual measurements is not informative with respect to sensitivity, whereas variance in their ratio is predictive of sensitivity, such that increasing the ratio of the aperture-to-focal length increases the sensitivity of the eye. We found significantly larger *A:f* ratios in *H. cinerea* (1.20 ± 0.05) than all other species, as *R. pipiens*, *O. pumilio*, and *M. viridis* have similar ratios (0.99 ± 0.06; 0.92 ± 0.01; and 1.00 ± 0.002, respectively; Figure 4e).

Photoreceptor outer segments are an additional critical optical dimension, as the probability of photon absorption is largely determined by their morphology. Figure 5a shows representative high magnification micrographs of rod outer segments from the four species. Overall, nocturnal species had significantly longer length (*l*) and wider diameter (*d*) outer segments compared to the diurnal species. Interestingly, intra-diel variance in photoreceptor dimensions was also
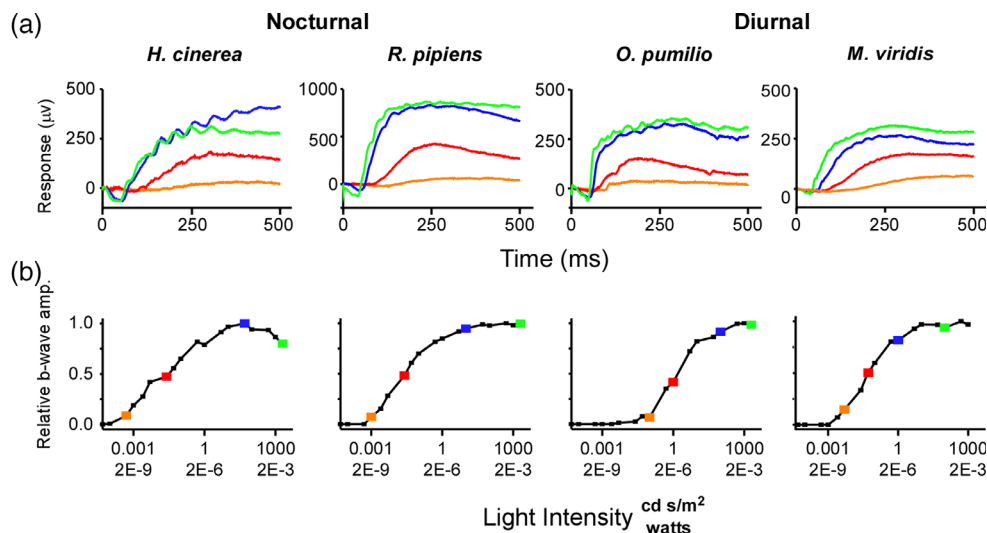
FIGURE 1   Example ERG waveforms and V-Log(*I*) curves for an individual of each species. Traces are the voltage response to a light stimulus for four of the light intensities across the stimulus intensity range (a). The amplitude of the b-wave is plotted in the V-Log(*I*) curves (b). Colors of the voltage traces correspond to the symbols on the V-Log(*I*) plots
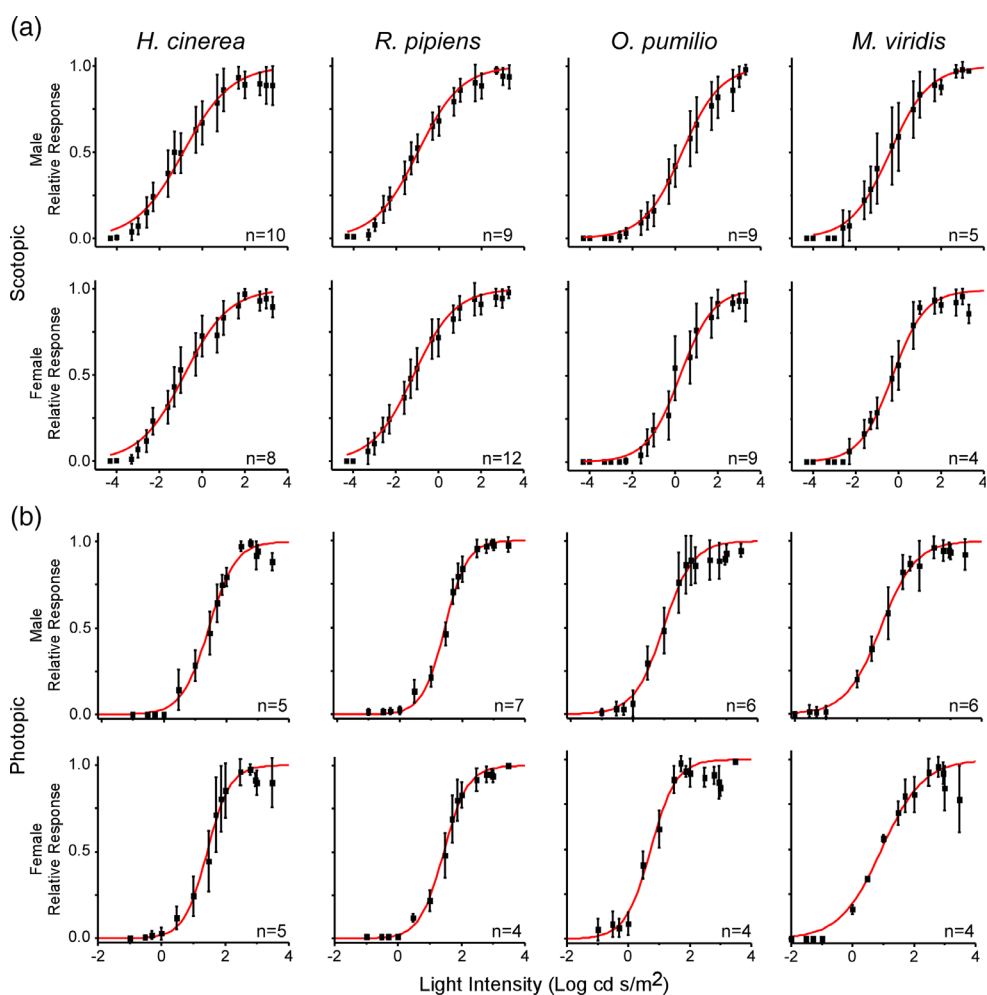
FIGURE 2   V-Log(*I*) curves showing mean ERG responses for each species under scotopic (a) and photopic (b) conditions. Each point represents the mean (±*SEM*) relative b-wave amplitude at each light intensity. Sample size (*n*) indicates the number of frogs used in each test. Males and females are separated into the upper and lower rows, respectively, for each condition. Red curves are the least-squares fit of the Boltzmann function to the entire population data. Note that Boltzmann function fits for each individual response were used to calculate threshold (i.e., light level eliciting 10% b-wave amplitude), slope, and dynamic range (Tables 1 and 2). *X*-axis scale differs in (a) and (b)

TABLE 1 Nocturnal versus diurnal ERG responses and optical anatomy

	Nocturnal		Diurnal		
	Mean ± SEM	n	Mean ± SEM	n	p
Scotopic ERG					
Thresh (log cd/m^2/s)	−3.12 ± 0.07	39	−1.72 ± 0.11	29	<.0001
Saturation (log cd/m^2/s)	1.18 ± 0.13	39	1.68 ± 0.16	29	.0164 n.s.
V-Log(I) slope	0.98 ± 0.03	39	0.77 ± 0.03	29	<.0001
Dynamic range (log cd/m^2/s)	4.30 ± 0.15	39	3.41 ± 0.12	29	<.0001
Photopic ERG					
Thresh (log cd/m^2/s)	0.64 ± 0.05	21	−0.18 ± 0.06	22	<.0001
Saturation (log cd/m^2/s)	2.25 ± 0.05	21	1.99 ± 0.09	22	.0215 n.s.
V-Log(I) slope	0.37 ± 0.02	21	0.38 ± 0.02	22	.0003
Dynamic range (log cd/m^2/s)	1.61 ± 0.07	21	2.17 ± 0.12	22	.0003
Optical anatomy					
Outer segment length (*l*) (µm)	49.99 ± 2.00	42	24.49 ± 1.00	44	<.0001
Outer segment diameter (*d*) (µm)	6.89 ± 0.70	43	4.42 ± 1.50	49	<.0001
Focal length (*f*) (mm)	3.43 ± 0.80	9	1.30 ± 0.68	12	<.0001
Pupil (*A*) (mm)	3.64 ± 0.68	9	1.23 ± 0.08	12	<.0001
Sensitivity (*S*)	16.13 ± 1.28	9	4.29 ± 0.94	12	<.0001

The left column is either the optical anatomical parameter or the characteristic of the V-Log(*I*) curves base on ERG b-wave amplitude. Subsequent columns are the nocturnal and diurnal species means (± *SEM*); sample sizes; *p* value for the general linear model comparison of nocturnal versus diurnal means. Alpha correction for multiple comparisons yields a significance value of 0.01, as each measurement is used in five comparisons (1 time between diel niche shown here; 3 times between species in Figure 3; 1 time between sexes in Table 3). n.s. denotes nonsignificant results after correction.

observed. *R. pipiens* photoreceptors were significantly larger than those of *H. cinerea* and *M. viridis* exhibited larger photoreceptors than *O. pumilio* (Figure 5b; Table 2).

Using these optical parameters in the Land equation and an absorption coefficient of 0.041 for frogs (Harosi & MacNichol Jr., 1974; Liebman, 1972; Warrant & Nilsson, 1998), sensitivity values were calculated for all of the eyes in which focal length and pupil diameter were measured. Note, however, that the calculation of each

eye's sensitivity used the average rod outer segment dimensions measured for each species. This method was used because while there is only one measure of *A* and *f* within each examined eye, sections of retina offered many rods from which to measure outer segment dimensions. Using this method, mean (±SE) optical sensitivities (*S*) in the nocturnal species were: *R. pipiens* 15.9 ± 2.0 and *H. cinerea* 16.4 ± 1.7. These were significantly greater than those for the diurnal species: *O. pumilio* 1.2 ± 0.03 and *M. viridis* 7.4 ± 0.03. Finally, the

TABLE 2 Interspecific variation in ERGs and optical anatomy

	Hyla cinerea Mean ± SEM	n	Rana pipiens Mean ± SEM	n	Oophaga pumilio Mean ± SEM	n	Mantella viridis Mean ± SEM	n
Scotopic ERG								
Threshold	−3.05 ± 0.12	18	−3.18 ± 0.08	21	−1.46 ± 0.11	18	−2.16 ± 0.14	11
Saturation	1.33 ± 0.19	18	1.05 ± 0.18	21	2.03 ± 0.16	18	1.12 ± 0.26	11
Slope	1.00 ± 0.05	18	0.96 ± 0.05	21	0.79 ± 0.04	18	0.75 ± 0.04	11
Dynamic range	4.38 ± 0.22	18	4.23 ± 0.20	21	3.49 ± 0.17	18	3.29 ± 0.16	11
Photopic ERG								
Threshold	0.62 ± 0.10	10	0.65 ± 0.05	11	−0.03 ± 0.05	10	−0.30 ± 0.08	12
Saturation	2.25 ± 0.08	10	2.24 ± 0.07	11	1.83 ± 0.16	10	2.12 ± 0.09	12
Dynamic range	1.63 ± 0.10	10	1.59 ± 0.10	11	1.86 ± 0.17	10	2.43 ± 0.14	12
Slope	0.37 ± 0.02	10	0.36 ± 0.02	11	0.42 ± 0.04	10	0.55 ± 0.03	12
Optical anatomy								
OS length (*l*) (µm)	43.04 ± 1.85	18	55.20 ± 1.90	24	18.66 ± 0.96	24	31.49 ± 0.92	20
OS diameter (*d*) (µm)	6.48 ± 0.18	18	7.18 ± 0.09	35	3.03 ± 0.14	23	5.65 ± 0.17	26
Focal length (*f*)(mm)	2.65 ± 0.23	4	4.05 ± 0.09	5	1.31 ± 0.03	6	1.28 ± 0.02	6
Pupil (*A*) (mm)	3.17 ± 0.26	4	4.02 ± 0.26	5	1.20 ± 0.02	6	1.27 ± 0.04	6
Sensitivity (*S*) (µm^2 sr)	16.40 ± 1.69	4	15.91 ± 2.05	5	1.19 ± 0.03	6	7.40 ± 0.03	6

The left column shows the measures from the V-Log(*I*) curves and optical anatomy. Subsequent columns are the mean (± *SEM*) and sample size for each measure from the four species of frogs. Threshold, saturation and dynamic range are reported in Log(cd s/m^2), as in the V-Log(*I*) curves. OS refers to rod outer segment.

TABLE 3 Comparison of male versus female ERG responses

	Male Mean $\pm$ SEM	Female Mean $\pm$ SEM	Male versus female p
Hyla cinerea			
Scotopic	n = 10	n = 8	
Thresh (log cd s/m^2)	−3.10 $\pm$ 0.19	−2.98 $\pm$ 0.13	.635
Saturation (log cd s/m^2)	1.33 $\pm$ 0.30	1.33 $\pm$ 0.25	.999
V-log(I) slope	1.01 $\pm$ 0.09	0.98 $\pm$ 0.04	.793
Dynamic range (log cd s/m^2)	4.43 $\pm$ 0.38	4.31 $\pm$ 0.19	.797
Photopic	n = 5	n = 5	
Thresh (log cd s/m^2)	0.52 $\pm$ 0.15	0.72 $\pm$ 0.12	.323
Saturation (log cd s/m^2)	2.34 $\pm$ 0.06	2.16 $\pm$ 0.14	.276
V-Log(I) slope	0.41 $\pm$ 0.04	0.33 $\pm$ 0.01	.049 n.s.
Dynamic range (log cd s/m^2)	1.82 $\pm$ 0.15	1.44 $\pm$ 0.05	.049 n.s.
Rana pipiens			
Scotopic	n = 9	n = 12	
Thresh (log cd s/m^2)	−3.18 $\pm$ 0.12	−3.18 $\pm$ 0.11	.979
Saturation (log cd s/m^2)	1.25 $\pm$ 0.24	0.90 $\pm$ 0.25	.339
V-Log(I) slope	1.01 $\pm$ 0.07	0.93 $\pm$ 0.06	.409
Dynamic range (log cd s/m^2)	4.43 $\pm$ 0.30	4.08 $\pm$ 0.28	.405
Photopic	n = 7	n = 4	
Thresh (log cd s/m^2)	0.66 $\pm$ 0.08	0.64 $\pm$ 0.07	.871
Saturation (log cd s/m^2)	2.23 $\pm$ 0.08	2.26 $\pm$ 0.13	.869
V-Log(I) slope	0.36 $\pm$ 0.03	0.37 $\pm$ 0.03	.835
Dynamic range (log cd s/m^2)	1.58 $\pm$ 0.14	1.62 $\pm$ 0.13	.836
Oophaga pumilio			
Scotopic	n = 9	n = 9	
Thresh (log cd s/m^2)	−1.60 $\pm$ 0.16	−1.32 $\pm$ 0.14	.204
Saturation (log cd s/m^2)	2.25 $\pm$ 0.22	1.80 $\pm$ 0.22	.157
V-Log(I) slope	0.88 $\pm$ 0.06	0.71 $\pm$ 0.03	.028 n.s.
Dynamic range (log cd s/m^2)	3.85 $\pm$ 0.28	3.12 $\pm$ 0.12	.029 n.s.
Photopic	n = 6	n = 4	
Thresh (log cd s/m^2)	0.04 $\pm$ 0.06	−0.13 $\pm$ 0.07	.118
Saturation (log cd s/m^2)	1.98 $\pm$ 0.23	1.60 $\pm$ 0.17	.272
V-Log(I) slope	0.44 $\pm$ 0.06	0.39 $\pm$ 0.05	.569
Dynamic range (log cd s/m^2)	1.94 $\pm$ 0.25	1.73 $\pm$ 0.23	.572
Mantella viridis			
Scotopic	n = 4	n = 5	
Thresh (log cd s/m^2)	−2.14 $\pm$ 0.24	−1.92 $\pm$ 0.12	.460
Saturation (log cd s/m^2)	1.37 $\pm$ 0.40	1.37 $\pm$ 0.30	.994
V-Log(I) slope	0.80 $\pm$ 0.04	0.75 $\pm$ 0.07	.546
Dynamic range (log cd s/m^2)	3.51 $\pm$ 0.19	3.28 $\pm$ 0.30	.519
Photopic	n = 6	n = 4	
Thresh (log cd s/m^2)	−0.32 $\pm$ 0.09	−0.50 $\pm$ 0.05	.143
Saturation (log cd s/m^2)	2.0 $\pm$ 0.12	2.40 $\pm$ 0.14	.070
V-Log(I) slope	0.53 $\pm$ 0.02	0.66 $\pm$ 0.04	.015 n.s.
Dynamic range (log cd s/m^2)	2.32 $\pm$ 0.09	2.89 $\pm$ 0.19	.015 n.s.

Columns are the optical parameter or V-Log(I) measurement of ERG b-waves; nocturnal and diurnal species means ($\pm$ SEM); sample sizes; p value for the general linear model comparison of means. Alpha correction for multiple comparisons yields a significance value of 0.01, as each measurement is used in five comparisons (1 time between diel niches; 3 times between species in Figure 3; 1 time between sexes here). n.s. denotes nonsignificant results after correction.

calculated sensitivity values strongly predict scotopic physiological thresholds, explaining nearly all of the variance (R^2 = 0.996; p < .005; Figure 6). Establishing this relationship in general, but for frogs in particular, is novel, as the linear relationship (slope = −0.110; intercept = −1.339 log cd s/m^2) allows for extrapolation of the retinal physiological threshold from simple measures of the optical anatomy.
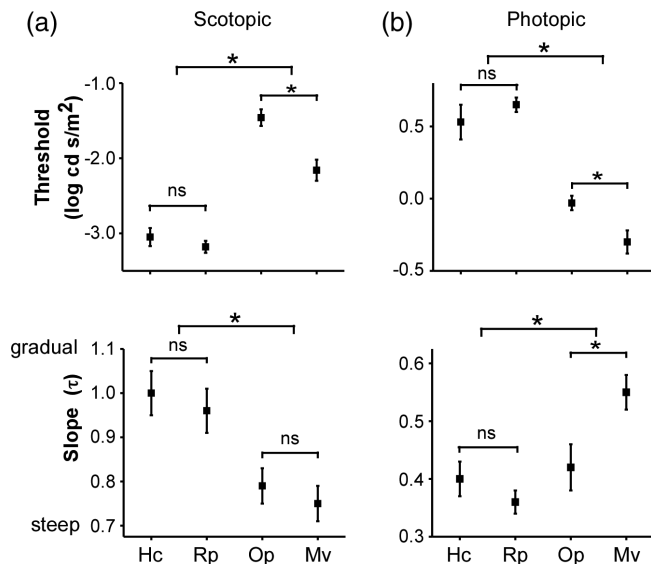
FIGURE 3 Within and between light niche (diurnal and nocturnal) comparisons of scotopic (a) and photopic (b) V-Log(I) mean thresholds and mean slopes. Data are listed in Tables 1 and 2. Asterisks denote statistical significance; n.s. not significant. Species names are abbreviated on the x-axes

4 | DISCUSSION

Although previously tested in insects (Frederiksen & Warrant, 2008), to the best of our knowledge, the present study represents the first attempt in vertebrates to correlate retinal physiological threshold and theoretical optical sensitivity across species, producing remarkable agreement and, in effect, calibrating the predictive capability of the

parameters in the Land equation to physiologically relevant light levels. Our choice taxa for this comparative work were anurans, which, since Cajal's work, have provided much of the fundamental knowledge on retinal function and eye morphology (Ewert & Arib, 1989; Fite, 1976; Llinás & Precht, 1976). Here, their use revealed the correlation between diel behavioral niche and retinal sensitivity, quantifying the relationship between optical anatomy and retina physiological sensitivity in nocturnal and diurnal frogs. This relationship's high R^2 (Figure 6) means that little else besides optical anatomy is needed to explain the variance in thresholds. That strong correlation notwithstanding, the scaling of the optical-to-physiological sensitivities was not equivalent, as threshold stimulus levels changed at ~0.11 the rate of optical sensitivity. There are no a priori predicted values for this relationship, however, as it was previously unmeasured in vertebrates and the units do not intuitively correlate to each other. Whereas optical sensitivity is essentially an area of the visual scene scaled to photoreceptor area, threshold here is the amount of luminance on a logarithmic scale required to elicit a 10% voltage response at one cell central from transduction. Because this latter metric is electrophysiological, at least one hypothesis for the different scaled change in stimulus levels at threshold relative to optical sensitivity is based on the mechanisms of transduction and neural transmission, each introducing their own scaling that varies in both space and time, which is not a factor in optical sensitivity. As noted above, an alternative approach to measuring this relationship was accomplished in insects, in which different species' optical sensitivities were compared to the size of neural responses at the same light intensity (Frederiksen & Warrant, 2008). Thus, response size was compared, rather than stimulus size at the threshold. The slope of that relationship (response size vs. optical
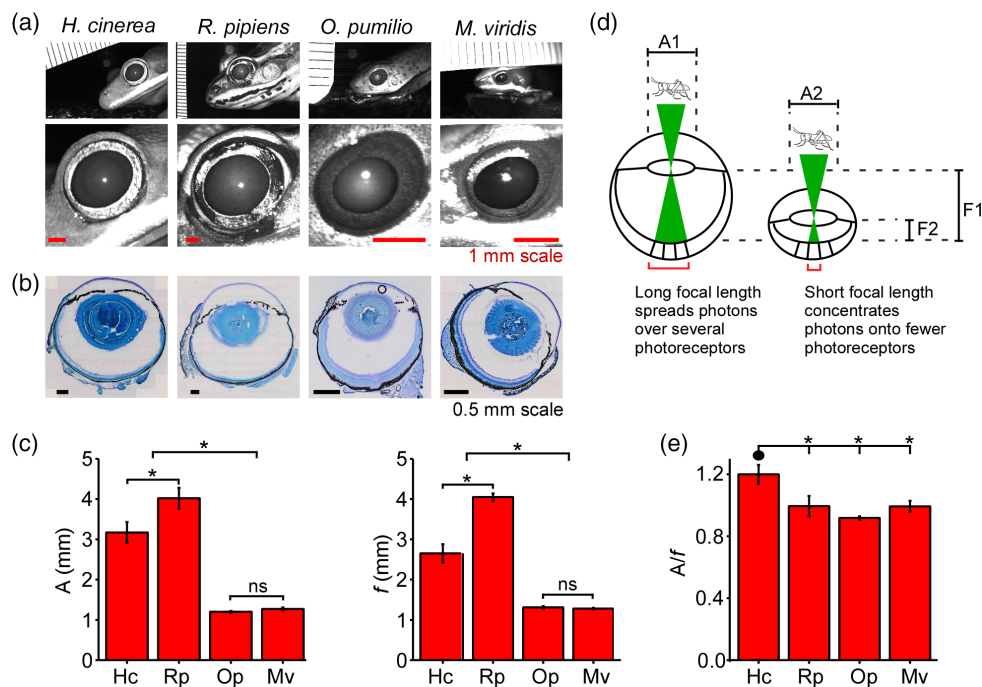
FIGURE 4 (a) Example infrared photographs of dilated pupils used to measure aperture size in *H. cinerea*, *R. pipiens*, *O. pumilio*, and *M. viridis* (left to right). Second row is magnification from above. (b) Flash frozen sections for each species at largest lens diameter used to measure focal distance. (c) Comparisons of mean aperture, *A*, and focal distance, *f*. Asterisks denote statistical significance ($p < .05$); n.s. not significant. Species names are abbreviated on the x-axes. (d) Illustration of the effect of A/f ratio. Large ratios focus more light onto fewer receptors, increasing sensitivity. (e) Comparisons of A/f ratio. Only *H. cinerea* differed from the other species
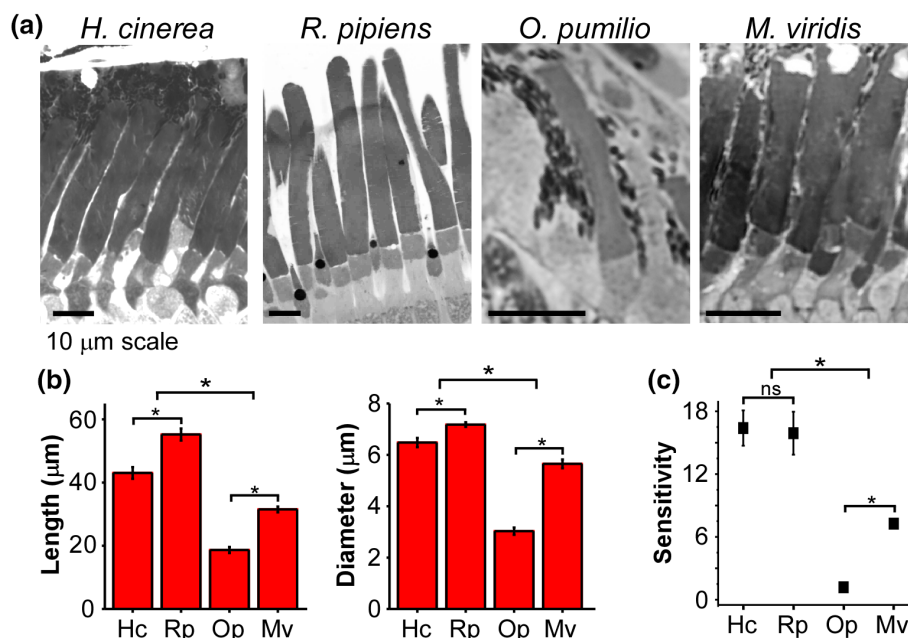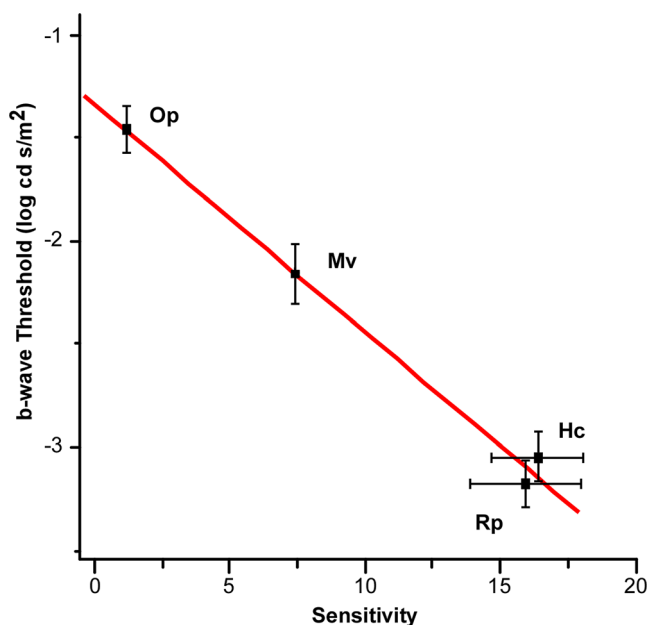
FIGURE 5 (a) High magnification light microscopy of rod outer segments. Micrographs of semithin plastic sections of the photoreceptors for each species. Scale bar = 10 μm. (b) Comparison of rod outer segment mean length and width across species. (c) Comparison of mean optical sensitivities calculated from the Land equation. Asterisks denote statistical significance ($p < 0.05$); n.s. not significant. Species names are abbreviated on the x-axes. Error bars are $\pm$ SEM

sensitivity) also differed from a 1:1 relationship by more than an order of magnitude, although some of that difference could be due to error from the lack of an extended light source (Frederiksen & Warrant, 2008). At present, with only two studies (insects and frogs) reporting the relationship between optical and physiological sensitivities, more

FIGURE 6 Relationship between theoretical optical sensitivity calculated using the Land equation versus b-wave threshold (i.e., light level eliciting 10% b-wave amplitude). Symbols are the mean ($\pm$SEM) for each species noted with initials. Line is a linear regression of the means providing prediction of luminance threshold given a particular optical sensitivity (slope = −0.110; intercept = −1.339; $p = .0041$; $R^2 = 0.996$)

data across taxa are needed to determine the extent to which the scaling of this relationship is universal or specialized to particular taxa with particular visual processing.

4.1 | Visual ecology and sensitivity

Selective pressure is expected on receiver sensitivity in animals that use vision under nocturnal or low light conditions where there may be 10^6-fold fewer photons than are available to diurnal animals. With regard to the eye's optical structure and retina, there are numerous examples of responses to selection from the photic environment, including changes in aperture, photoreceptor size, and focal distance, traits that are the focus of this paper and predicted from Equation (1), the Land equation (Cronin et al., 2014; Warrant, 2017; Warrant & Dacke, 2016). Such selection is, of course, most expected in taxa that are strictly limited to a particular light niche, such as the low photon environments of the deep sea (Cronin et al., 2014). For example, when considering adaptations across the entire retina, lanternfish have theoretical optical sensitivity approximately two orders of magnitude greater than the diurnal human eye (de Busserolles & Marshall, 2017; Warrant & Locket, 2004). By virtue of their circadian ecology, our subject species experience temporal, not spatial, constraints in photon availability (as opposed, e.g., to species which live at depths constrained in photon availability by the spatial effects of light distribution, but not by the diel cycle). Specifically, categorization of nocturnal and diurnal was based on mating behavior and visual aposematism, such that diurnal species call during the day time, and nocturnals primarily during and after sunset (Garton & Grandon, 1975; Gerhardt, Daniel, Perrill, & Schramm, 1987; Larson, 2004; Prohl, 2003; Vences, Glaw, & Bohme, 1999). Thus, because this categorization was based on certain temporally limited behavior patterns, the animals' eyes

could also still function in the opposite light condition (i.e., the opposite phase of the diel cycle). This would potentially limit the differences in selection on traits affecting sensitivity. Nevertheless, our categorization of light niche did indeed segregate visual traits, as our study revealed evidence for differing selective pressure on nocturnal versus diurnal frogs' optical and physiological sensitivity. With regard to optical sensitivity, the data revealed which anatomical parameters in Equation (1) (Table 1) yielded higher sensitivity in nocturnal frogs. For example, although pupil aperture is larger in nocturnal frogs, the focal distance largely scaled with aperture size across species (*H. cinerea* excepted), meaning there appeared to be little effect on the range of optical sensitivities due to changing pupil size in these eyes. That is, a larger eye is not more sensitive per se if there is isometric scaling of A and f (creating a near constant inverse of the f-stop across three of the four species). For these frogs, differences in optical sensitivity thus appear to depend more on the dimensions of the rod outer segments. Both rod diameter (d) and length (l) were significantly larger in the nocturnal animals, resulting in calculations of greater optical sensitivity (Table 1). Note that a statistical analysis of these parameters' effects on *individual variance* in sensitivity was not possible, as dimensions of the outer segments were not calculated per individual eye (i.e., like A and f were). Instead, means of d and l were used for each species' calculation of sensitivity.

Control of changes in sensitivity through changes in receptor dimensions is not limited to the photoreceptor outer segments, as increased sensitivity could result from increased effective collective area through spatial summation (Stockl, O'Carroll, & Warrant, 2016; Stockl, Ribi, & Warrant, 2016), such as at the ganglion cell layer in the vertebrate eye (de Busserolles & Marshall, 2017). Anatomical data in other frog species show distal-to-central convergence across the outer plexiform layer potentially enabling summation (Dowling, 1968). Although our data cannot directly address summation, based on the strong correlation between optical and physiological sensitivities, our data indirectly suggest that for these species there is no difference in the amount of summation. Indeed, the optical-to-physiological relationship in Figure 6 leads to the following conditional: if the per rod prediction of the Land equation explains threshold with similar accuracy across species, then the collecting areas measured for each species and employed by the equation must be equally accurate. With respect to collecting area, equal accuracy could result from two possibilities: (a) the per rod collecting area is accurate and there is no convergence at the bipolar cells; (b) there is convergence to create larger collecting areas, but that this convergence is identical in the four species. Figure 6 shows that the optical sensitivity, which is calculated as the per rod sensitivity in Equation (1), explains nearly all of the variance in b-wave threshold ($R^2 = 0.996$). Had any of these species expressed larger effective collecting areas due to a greater amount of summation in the inner nuclear layer, for example, the ERG b-wave threshold would not have been explained by the linear fit and would have been lower (on the y-axis) than a linear function (Figure 6). The inference notwithstanding, experiments here were at a gross level and more direct testing of individual bipolar cell receptive fields is needed to quantify the extent to which physiological summation affects threshold in the frog inner retina.

4.2 | Comparing optical sensitivity in frogs to other taxa

A large range of optical sensitivities has been calculated across species from different light niches (Warrant & Nilsson, 1998). In general, nocturnal eyes exhibit optical sensitivities from approximately 2 to 100 μm^2 sr, with greater sensitivity (>1,000) for those animals in photon-starved (e.g., deep sea) environments. In contrast, sensitivities in diurnal species' eyes range roughly from ~0.004 to 2 μm^2 sr. Three of our subject species fit well into these ranges. Both nocturnal frogs, *H. cinerea* and *R. pipiens*, have calculated optical sensitivities near 16 μm^2 sr, suggesting that these eyes indeed function in low light processing. The diurnal *O. pumilio* (Prohl & Hodl, 1999; Summers et al., 1999) matches sensitivity in other day active species with its calculated sensitivity near 1 μm^2 sr. Interestingly, calculated sensitivity in *M. viridis* is conspicuously intermediate to the other species here and those measured in other studies (Warrant & Nilsson, 1998). When considered alone, such an unusual optical sensitivity calculation could have resulted from a methodological error in one of the anatomical measurements. This is unlikely, however, as physiological thresholds from ERGs independently confirm this frog's intermediate sensitivity to light stimuli. Taken together, the data suggest that these aposematic frogs may not be strictly diurnal or at least inhabit lower light environments than *O. pumilio*. Ecologically, both species are diurnal, aposematic frogs, which would seem to indicate that they inhabit similar light environments, making the difference particularly intriguing.

How do measurements of optical sensitivity and threshold here compare to those in other frogs? To the best of our knowledge, there are no other anurans in which both the optical anatomy and some form of the retinal threshold have been measured together. However, other histological and behavioral measures are in good agreement. For example, Aho, Donner, and Reuter (1993) found *R. pipiens* rod outer segment dimensions to be 53.0 × 7.3 μm, quite close to those here (55.2 × 7.18 μm). In addition, they measured jumping thresholds from −2 to −2.7 log(Rh* per second), overlapping the 10% b-wave threshold measured here, −2.37 log(Rh* per second); units converted following Saszik, Robson, & Frishman (2002). Optical anatomy and scotopic response thresholds have also been measured in different species of toads (Bufonidae; *Bufo*): *B. americanus* and *B. bufo*, respectively. Based on their movement and breeding behavior, both of these species are nocturnal (Gatz, 1981; Gittins, Parker, & Slater, 1980; Sullivan, 1992) and the combination of the two measures could be used to test the relationship established here for optical sensitivity and physiological threshold (Figure 6). Data for behavioral and physiological thresholds from independent studies on *B. bufo* are in good agreement, showing thresholds near −4.5 log cd s/m² (Aho, Donner, Helenius, Larsen, & Reuter, 1993; Larsen & Pedersen, 1981). Based on our data, this threshold would predict an optical sensitivity near 21 μm^2 sr. However, optical sensitivity for toads has been based on anatomical measurements in *B. americanus* by Mathis, Schaeffel, and Howland (1988), which yielded a sensitivity of only 2.41, quite low for the nocturnal range of sensitivities measured here. Specifically, this combination of threshold and sensitivity (between species) would fall well below the function in Figure 6. While this mismatch in threshold and optical sensitivity could be due to the combination measurements

from different species, we suggest that it may also be due to mis-measured rod diameter (2.5 μm) in *B. americanus*. Rod diameter in other toads ranges from ~5.2 to 8.45 μm (Hailman, 1976) meaning that the spatial sampling resolution of the 7 μm histological sections used by Mathis et al. (1988) could easily cut outer segments at points smaller than at their widest point. It is for this reason that our study used two independent methods to confirm outer segment diameter: thin (1 μm) sections in plastic and DIC microscopy in thicker sections to allow for adjustment of the focal plane to the widest outer segment diameter. These methods yielded consistent results and, at least for *R. pipiens*, produced similar measurements to that in other *Rana* species (6.2–8.5 μm; Tsukamoto, 1987; Zhang et al., 2013). Thus, we suggest that the optical sensitivity reported for *Bufo* should be reexamined.

4.3 | Scotopic ERG thresholds and behavior

As a consequence of low photon availability, much of the behavior of nocturnal animals is mediated by sensory modalities other than light (Bradbury & Vehrencamp, 1998). Frogs are no exception, as most are nocturnal and use elaborate acoustic displays and auditory processing to mediate reproductive behavior (Gerhardt & Huber, 2002; Wells, 2007). These behavior patterns notwithstanding, vision is still used by nocturnal frogs in orientation, prey capture, predator avoidance, and communication (Ewert, 1976; Farris & Taylor, 2016; Gomez et al., 2009; Rosenthal, Rand, & Ryan, 2004; Taylor, Klein, Stein, & Ryan, 2011). Consistent with behavioral measures in other studies, scotopic thresholds measured here show that nocturnal light availability is quite sufficient to employ visual processing in these behavior patterns. For example, when converted to log cd/m^2 (for consistency with this study), light levels on the forest floor during the lunar cycle range from approximately −1.6 to 0.21 log cd/m^2 (Cummings, Bernal, Reynaga, Rand, & Ryan, 2008). This range is above isomerization thresholds (Copenhagen, Hemila, & Reuter, 1990) and more than one order of magnitude greater than scotopic thresholds in *H. cinerea* and *R. pipiens* (which are approximately −3 log cd s/m^2; Table 2). This natural light range also stimulates the retina at the steepest part of the V-Log(I) curve (Figure 2), meaning dark-adapted retina are well matched to function in intensity discrimination under nocturnal conditions. It is worth noting, however, that scotopic and photopic V-Log(I) curves do overlap at the higher end of the scotopic curves, meaning some of the steep parts of the scotopic response could be a mix of rod and cone vision (mesopic). These V-Log(I) curves nevertheless provide guidance for consideration of how optimally matched visual systems may be to light levels under natural and artificial conditions (Buchanan, 2006; Grant, Halliday, & Chadwick, 2013).

4.4 | Photopic thresholds and cone vision

As expected, for all species, photopic thresholds increased relative to those measured under scotopic conditions. Importantly, from a methodological point of view, photopic thresholds were not simply a linear shift of the scotopic thresholds, which could have resulted from an adaptation of rods. Instead, the relative differences in photopic thresholds were changed, as nocturnal frogs were now less sensitive.

There are several important inferences from these results. First, use of background illumination at a level common to the forest floor (Jaeger & Hailman, 1981) when diurnal frogs are active appears sufficient to reduce rod based processing, as photopic curves saturated above scotopic saturation and only overlapped the high end of the scotopic dynamic range. Furthermore, had rods still been largely utilized in these conditions then the optical parameters in Equation (1) would have likely mediated relative sensitivity like that in scotopic conditions and resulted in lower thresholds in the nocturnal species. The reverse of these results (i.e., from scotopic conditions) suggests that rod collecting area, a large determinant of sensitivity compared to the less variant *A:f* ratio, appears less relevant under daylight condition, presumably allowing for the cone-based vision to dominate. Second, from an ecological point of view, this reduction of rod-based vision by moving the curves to intensities at the top of the scotopic dynamic range means that under natural diurnal illumination, visual behavior in these frogs is potentially mediated by cones. This conclusion emphasizes the importance of defining cone mosaics for parsing the significance of visual signaling variance. Finally, if photopic responses accurately reflect sensitivity in cones, then the cone thresholds in diurnal species are sufficient for mediating processing throughout the day and on the forest floor (Jaeger & Hailman, 1981; Liebau, Eisenberg, & Esser, 2015).

5 | CONCLUSION

Despite their long history of use in visual system research, understanding of how anuran eyes have adapted to different light environments is still incomplete. Beyond a need for comparative work in anurans, there was also an incomplete understanding of the relationship between differences in optical anatomy and actual physiological thresholds. This study helped to address both of these issues, showing clear interspecific adaptations to visual ecology, while also generating a null hypothesis that predicts the general relationship between optical adaptations and physiological sensitivity.

CONFLICT OF INTEREST

The authors have no conflicts of interest.

ORCID

Hamilton E. Farris https://orcid.org/0000-0002-7392-5819

REFERENCES

Aho, A. C., Donner, K., Helenius, S., Larsen, L. O., & Reuter, T. (1993). Visual performance of the toad (*Bufo bufo*) at low light levels: Retinal ganglion cell responses and prey-catching accuracy. *Journal of Comparative Physiology A*, 172, 671–682.

Aho, A. C., Donner, K., & Reuter, T. (1993). Retinal origins of the temperature effect on absolute visual sensitivity in frogs. *The Journal of Physiology*, 463, 501–521.

Bradbury, J. W., & Vehrencamp, S. L. (1998). *Principles of animal communication*. Sunderland, MA: Sinauer Associates Inc.

Buchanan, B. W. (2006). Observed and potential effects of artificial night lighting on anuran amphibians. In C. Rich & T. Longcore (Eds.), *Ecological consequences of artificial night lighting* (pp. 190–220). Washington, DC: Island Press.

Copenhagen, D. R., Hemila, S., & Reuter, T. (1990). Signal transmission through the dard-adapted retina of the toad (*Bufo marinus*). *Journal of General Physiology*, 95, 717–732.

Cronin, T. W., Johnsen, S., Marshall, N. J., & Warrant, E. J. (2014). *Visual Ecology*. Princeton, NJ: Princeton University Press.

Cummings, M. E., Bernal, X. E., Reynaga, R., Rand, A. S., & Ryan, M. J. (2008). Visual sensitivity to a conspicuous male cue varies by reproductive state in *Physalaemus pustulosus* females. *Journal of Experimental Biology*, 211, 1203–1210.

de Busserolles, F., & Marshall, N. J. (2017). Seeing in the deep-sea: Visual adaptations in lanternfishes. *Philosophical Transactions of the Royal Society, B: Biological Sciences*, 372, 20160070.

Donner, K. O., & Reuter, T. (1976). Visual pigments and phtoreceptor functions. In R. Llinas & W. Precht (Eds.), *Frog Neurobiology* (pp. 251–277). New York: Springer.

Dowling, J. E. (1968). Synaptic organization of the frog retina: An electron microscopic analysis comparing the retinas of frogs and primates. *Proceedings of the Royal Society of London, Series B: Biological Sciences*, 170, 205–228.

Duellman, W. E., & Trueb, L. (1994). *Biology of amphibians*. Baltimore, MD: The Johns Hopkins University Press.

Dusenbery, D. (1992). *Sensory ecology*. New York: W. H. Freeman.

Eguchi, E., & Horikoshi, T. (1984). Comparison of stimulus-response (V-log I) functions in five types of lepidopteran compound eyes (46 species). *Journal of Comparative Physiology A*, 154, 3–12.

Endler, J. A. (1992). Signals, signal conditions and the direction of evolution. *American Naturalist*, 139, S125–S153.

Ewert, J.-P. (1976). The visual system of the toad: Behavioral and physiological studies on a pattern recognition system. In K. V. Fite (Ed.), *The amphibian visual system: A multidisciplinary approach* (pp. 141–201). New York: Academic Press.

Ewert, J.-P., & Arbib, M. A. (1989). *Visuomotor Coordination*. New York: Plenum Press.

Farris, H. E., & Taylor, R. C. (2016). Mate searching animals as model systems for understanding perceptual grouping. In M. A. Bee & C. T. Miller (Eds.), *Psychological mechanisms in animal communication* (pp. 89–118). New York: Springer.

Fite, K. V. (1976). *The amphibian visual system*. New York: Academic Press.

Frederiksen, R., & Warrant, E. J. (2008). The optical sensitivity of compound eyes: Theory and experiment compared. *Biology Letters*, 4, 745–747.

Garton, J. S., & Grandon, R. A. (1975). Reproductive ecology of the green treefrog, *Hyla cinerea*, in southern Illinois (Anura: Hylidae). *Herpetologica*, 31, 150–161.

Gatz, A. J. (1981). Non-random mating by size in american toads, *Bufo americanus*. *Animal Behaviour*, 29, 1004–1012.

Gerhardt, H. C., Daniel, R. E., Perrill, S. A., & Schramm, S. (1987). Mating behaviour and male mating success in the green treefrog. *Animal Behaviour*, 35, 1490–1503.

Gerhardt, H. C., & Huber, F. (2002). *Acoustic communication in insects and anurans*. Chicago, IL: University of Chicago.

Gittins, S. P., Parker, A. G., & Slater, F. M. (1980). Population characteristics of the common toad (*Bufo bufo*) visiting a breeding site in mid-Wales. *Journal of Animal Ecology*, 49, 161–173.

Gomez, D., Richardson, C., Lengagne, T., Plenet, S., Joly, P., Lena, J. P., & Thery, M. (2009). The role of nocturnal vision in mate choice: Females prefer conspicuous males in the European tree frog (*Hyla arborea*). *Proceedings of the Biological Sciences*, 276, 2351–2358.

Grant, R., Halliday, T. R., & Chadwick, E. (2013). Amphibians' response to the lunar synodic cycle—a review of current knowledge, recommendations, and implications for conservation. *Behavioral Ecology*, 24, 53–62.

Hailman, J. P. (1976). Oildroplets in the eyes of adult anuran amphibians: A comparative survey. *Journal of Morphology*, 148, 453–468.

Harosi, F. I., & MacNichol, E. F., Jr. (1974). Visual pigments of goldfish cones. Spectral properties and dichroism. *The Journal of General Physiology*, 63, 279–304.

Jaeger, R. G., & Hailman, J. P. (1981). Activity of neotropical frogs in relation to ambient light. *Biotropica*, 13, 59–65.

Land, M. F. (1981). Optics and vision in invertebrates. In H. Autrum (Ed.), *Handbook of sensory physiology* (pp. 471–592). Berlin: Springer.

Land, M. F., & Nilsson, D.-E. (2002). *Animal Eyes*. Oxford: Oxford University Press.

Larsen, L. O., & Pedersen, J. N. (1981). The snapping response of the toad, *Bufo bufo*, towards prey dummies at very low light intensities. *Amphibia-Reptilia*, 2, 321–327.

Larson, K. A. (2004). Advertisement call complexity in northern leopard frogs, *Rana pipiens*. *Copeia*, 2004(3), 676–682.

Liebau, A., Eisenberg, T., & Esser, K. H. (2015). The scotopic and photopic visual sensitivity in the nocturnal tree frog *Agalychnis callidryas*. *Journal of Comparative Physiology A*, 201, 1035–1041.

Liebman, P. A. (1972). Microspectrophotometry of photoreceptors. In H. J. A. Dartnall (Ed.), *Photochemistry of vision. Handbook of sensory physiology* (Vol. 7/1, pp. 481–528). Berlin: Springer.

Llinás, R., & Precht, W. (1976). *Frog neurobiology: A handbook*. Berlin: Springer.

Mathis, U., Schaeffel, F., & Howland, H. C. (1988). Visual optics in toads (*Bufo americanus*). *Journal of Comparative Physiology A*, 163, 201–213.

Miller, R. F., & Dowling, J. E. (1970). Intracellular responses of the Muller (glial) cells of mudpuppy retina: Their relation to b-wave of the electroretinogram. *Journal of Neurophysiology*, 33, 323–341.

Nascimento, S. M., Amano, K., & Foster, D. H. (2016). Spatial distributions of local illumination color in natural scenes. *Vision Research*, 120, 39–44.

Prohl, H. (2003). Variation in male calling behviour and relation to male mating success in the strawberry poison frog (*Dendrobates pumilio*). *Ethology*, 109, 273–290.

Prohl, H., & Hodl, W. (1999). Parental investment, potential reproductive rates, and mating system in the strawberry dart-poison frog, *Dendrobates pumilio*. *Behavioral Ecology and Sociobiology*, 46, 215–220.

Pugh, E. N., Falsini, B., & Lyubarsky, A. L. (1998). The origin of the major rod- and cone-driven components of the rodent electroretinogram and the effect of age and light-rearing history on the magnitude of these components. In T. P. Williams & A. B. Thistle (Eds.), *Photostasis and related phenomena* (pp. 93–128). New York: Springer.

Robson, J. G., & Frishman, L. J. (1998). Dissecting the dark-adapted electroretinogram. *Documenta Ophthalmologica*, 95, 187–215.

Rosenthal, G. G., Rand, A. S., & Ryan, M. J. (2004). The vocal sac as a visual cue in anuran communication: An experimental analysis using video playback. *Animal Behaviour*, 68, 55–58.

Saszik, S. M., Robson, J. G., & Frishman, L. J. (2002). The scotopic threshold response of the dark-adapted electroretinogram of the mouse. *The Journal of Physiology*, 543, 899–916.

Schaefer, H.-C., Vences, M., & Veith, M. (2002). Molecular phylogeny of Malagasy poison frogs, genus *Mantella* (Anura:Mantellidae): Homoplastic evolution of colour pattern in aposematic amphibians. *Organisms, Diversity and Evolution*, 2, 97–105.

Stockl, A. L., O'Carroll, D. C., & Warrant, E. J. (2016). Neural summation in the hawkmoth visual system extends the limits of vision in dim light. *Current Biology*, 26, 821–826.

Stockl, A. L., Ribi, W. A., & Warrant, E. J. (2016). Adaptations for nocturnal and diurnal vision in the hawkmoth lamina. *Journal of Comparative Neurology*, 524, 160–175.

Sullivan, B. K. (1992). Sexual selection and calling behavior in the American toad. *Copeia*, 1992, 1–7.

Summers, K., Symula, R., Clough, M., & Cronin, T. (1999). Visual mate choice in poison frogs. *Proceedings of the Biological Sciences*, 266, 2141–2145.

Taylor, R. C., Klein, B. A., Stein, J., & Ryan, M. J. (2011). Multimodal signal variation in space and time: How important is matching a signal with its signaler? *Journal of Experimental Biology, 214*, 815–820.

Tsukamoto, Y. (1987). Morphometrical features of rod outer segments in relation to visual acuity and sensitivity in the retina of *Rana catesbeina*. *Zoological Science, 4*, 233–242.

Vences, M., Glaw, F., & Bohme, W. (1999). A review of the genus *Mantella* (Anura, Ranidae, Mantellinae): Taxonomy, distribution and conservation of the Malagasy poinson frogs. *Alytes, 17*, 3–72.

Walls, G. L. (1942). *The vertebrate eye and its adaptive radiation*. New York: Hafner Publishing.

Warrant, E., & Dacke, M. (2011). Vision and visual navigation in nocturnal insects. *Annual Review of Entomology, 56*, 239–254.

Warrant, E., & Dacke, M. (2016). Visual navigation in nocturnal insects. *Physiology (Bethesda, Md.), 31*, 182–192.

Warrant, E. J. (2017). The remarkable visual capacities of nocturnal insects: Vision at the limits with small eyes and tiny brains. *Philosophical Transactions of the Royal Society, B: Biological Sciences, 372*, 20160063.

Warrant, E. J., & Johnsen, S. (2013). Vision and the light environment. *Current Biology, 23*, R990–R994.

Warrant, E. J., & Locket, N. A. (2004). Vision in the deep sea. *Biological Reviews of the Cambridge Philosophical Society, 79*, 671–712.

Warrant, E. J., & Nilsson, D. E. (1998). Absorption of white light in photo-receptors. *Vision Research, 38*, 195–207.

Wells, K. D. (2007). *The ecology and behavior of amphibians*. Chicago, IL: The University of Chicago Press.

Zar, J. H. (1999). *Biostatistical analysis*. Upper Saddle River, NJ: Prentice-Hall Inc.

Zhang, P., Zhou, H., Chen, Y.-G., Liu, Y.-F., Qu, L.-H., & Kjer, K. (2005). Mitogenomic perspectives on the origin and phylogeny of living amphibians. *Systematic Biology, 54*, 391–400.

Zhang, Q. X., Lu, R. W., Messinger, J. D., Curcio, C. A., Guarcello, V., & Yao, X. C. (2013). In vivo optical coherence tomography of light-driven melanosome translocation in retinal pigment epithelium. *Scientific Reports, 3*, 2644.